Recent experiments in the HT-7 superconducting tokamak

Baonian Wan 1), Zhongyong Chen 1), Youwen Sun 1), Guosheng Xu 1), Jiangang Li 1), Hongyu Bai 1), Bojiang Ding 1), V. Chan 9), Junling Chen 1), Peng Fu 1), Xiang Gao 1), K. Gentle 8), Xianzu Gong 1), Quangui Guo 2), Xuemao Guo 1), Shiying He 1), Yexi He 7), Jianshen Hu 1), Liqun Hu 1), H. Huang 8), Jun Huang 1), Yiyun Huang 1), Yanxin Jie 1), L. Lao 9), Guiming Li 1), Hua Li 1), Bili Ling 1), Shiyue Ling 1), Fukun Liu 1), Haiqing Liu 1), Guangnan Luo 1), Jiarong Luo 1), Nanchan Luo 1), Jianshan Mao 1), Yuzhou Mao 1), S.Morita 11), Zhenrong Ouyang 1), P. Philippe 8), Jinping Qian 1), Chenming Qing 1), Pingjian Qing 1), W. Rowan 8), Jiafang Shan 1), Biao Shen 1), Yuejiang Shi 1), K.Tanaka 10), K.Toi 10), Huazhong Wang 1), Linshen Wang 1), Long Wang 6), Xiaoming Wang 1), T. Watari 10), Yizi Wen 3), Zhenwei Wu 1), Bingjia Xiao 1), Jikang Xie 1), Xiaoyuan Xu 4), Longwen Yan 5), Qingwei Yang 5), Yu Yang 1), Chanxuan Yu 3), Junyu Zhao 1), Yanping Zhao 1), Xianmei Zhang 4), Xiaodong Zhang 1), Qing Zhou 1), and the HT-7 team 1)

1) Institute of Plasma Physics, Chinese Academy of Sciences, Hefei, China
2) Institute of Carbon Chemistry, Chinese Academy of Sciences, Taiyuan, China
3) University of Science and Technology of China, Hefei, China
4) East China University of Science and Technology, Shanghai, China.
5) Southwest Institute of Physics, Chengdu, China
6) Institute of Physics, Chinese Academy of Sciences, Beijing, China
7) Tsinghua University, Beijing, China
8) Fusion Research Center, UT at Austin, USA
9) General Atomic, San Diego, USA
10) National Institute for Fusion Sciences, Toki, Japan

e-mail contact of main author: bnwan@ipp.ac.cn

Abstract: Since the last IAEA meeting, experiments and system modification in the HT-7 tokamak focused on long pulse discharges based on lower hybrid current drive (LHCD) under different scenarios to support the EAST project both physically and technically. The long pulse discharges at the level of Ip~60 kA, $n_e(0)\sim0.8\text{-}1\times10^{19}/m^3$ has been extended to longer than 6 minutes using about 150kW of LHCD only, which are the new records of both the pulse length and injected energy in HT-7. A new steady-state AC operation mode has been demonstrated up to 53 s in ohmic plasmas and 30s in LHCD plasmas at the level of Ip=100-125kA, $n_e(0)\sim1.5\text{-}2.5\times10^{19}/m^3$. The relevant physics concerning on the lower hybrid current drive efficiency, MHD instability, conversion efficiency of LHW to poloidal energy t and dynamics of runaway electrons were studied. Radial propagation of electrostatic turbulence and intermittently occurring large-scale coherent structures were measured using the Langmuir probe arrays to study the turbulent transport in the plasma peripheral region.

1. Introduction

The achievement and control of steady-state fusion plasma is one of major efforts of tokamak physics for the next step. EAST (Experimental Advanced Superconducting Tokamak) is a mega-ampere full superconducting tokamak, which is aimed at steady-state operation with the shaped plasma cross-section [1,2]. The first engineering of the EAST device was performed successfully in March 2006 after five year's construction. The first plasma of EAST has been successfully achieved in September of 2006. Steady-state plasmas of EAST will be sustained by intensive use of radio frequency heating and current drive. The physics and technologies of long pulse operation with non-inductive current drive are essential basis for EAST. The institute of plasma physics, Chinese Academy of Sciences (IPP/CAS or ASIPP) has EAST as new project and simultaneous the HT-7 superconducting tokamak in operation. HT-7 provides us a good opportunity to do those investigations needed for EAST. In last two years, HT-7 focused on long pulse discharges based on lower hybrid current drive to support the EAST project both physically and technically.

HT-7 is a circular cross-section limiter tokamak (R=1.22 m, a= 0.27 m, B_{max}= 2.5 T) with the superconducting toroidal magnets and water cooled poloidal magnets, which is capable of continuous operation. The experiments have been conducted in predominantly deuterium target plasmas with a toroidal magnetic field B_T = 1.5-2.0 T, plasma currents I_p = 50-250 kA and central line-averaged electron densities $\bar{n}_e(0)$ = 0.5-6.0×10^{19} m^{-3}. One of the main efforts of the HT-7 superconducting tokamak is directed to long pulse discharges. HT-7 is thus equipped with a set of full actively cooled limiters and a heating and current drive capability based on high power RF systems connected to actively cooled antennas. The steady-state plasma operation is realized by intensive use of the lower hybrid current drive (LHCD). Significant progress in steady-state physics and technology has been achieved on the Tore-Supra, Triam-1M and HT-7 tokamaks in the last few years [3-7]. In Tore Supra, fully non-inductive plasma discharges have been sustained for up to 6 min 18 sec after a series of key technologies related to long pulse discharge has been established. TRIAM-1M has achieved a world record for discharge duration of 5 h 16 min, which aims directly at 'day long operation'. Significant progress has been also made at HT-7, in terms of plasma duration 4 minutes in 2004 and more recently up to 5 min 6 sec in 2005 with injected energy > 40MJ.

All these long pulse experiments addressed the importance of key technologies and physics of non-inductive current drive, particle control, actively cooled PFCs, diagnostics and real-time plasma control, which needed by next generation of steady-state superconducting tokamak experiments such as EAST, ITER. The runaway electrons may be produced in the LHCD plasma and low density plasmas and causes damage of the in-vessel components. They become particularly harmful for long pulse plasmas due to the heat accumulation by impinging on the in-vessel components. The effect of the runaway electrons when they impinge on the vessel walls or plasma facing components is strongly dependent on the energy gained in the electric field. The knowledge of the energy that can be reached by runaway electrons constitutes an essential tool to estimate the effect. In order to obtain detailed information on the dynamics of a runaway beam and the interaction of edge runaways with magnetic field ripple simultaneously, the runaway electrons have been measured recently in combination with hard x-ray detectors and a thermographic camera in the HT-7 tokamak.

As a medium-sized, circular cross-section tokamak, HT-7 is very suitable for the study of plasma turbulence. And the plasma temperature in the edge region is not too high, Langmuir probe can be applied. Specially shaped probe arrays can present detailed information about the structures and properties of plasma turbulence. In the recent two years the plasma edge group on HT-7 was devoted to the study of the turbulence structures and their propagation across magnetic surfaces.

The paper is organized as follows: Section 2 describes the general experimental conditions including some of most important system modification needed for long pulse discharges. In section 3 the physics of LHCD including the MHD instability are discussed. The control and operation of long pulse discharges in two operation scenarios are reported in section 4. The behaviors of run away electrons are presented in section 5. The brief results of the edge turbulence investigation is given in section 6 followed by a summary and conclusion in section 7.

2. Experimental conditions

In 2003, long pulse plasma discharges were obtained for duration of 60 seconds with two actively water-cooled full poloidal limiters on HT-7. The duration of the plasma discharges was mainly limited by an uncontrolled density increase. Correlation between density increase and the temperature of the graphite tiles on the limiter and liners confirmed that this increase was attributed to out-gassing from the limiter surface, which accumulated a lot of heat from the plasmas. New top-bottom flat toroidal belt limiters with high heat removing capacity were installed during the campaign in 2004 to replace the old poloidal limiters. The limiters with total surface area of 1.7 m^2 toroidally covered 265^o at top and 285^o at bottom respectively, which skipped the top and bottom ports for diagnostics [8]. CuCr was used as heat sink and doped graphite title with SiC gradient coating were bolted on the heat sink through an interlayer of a flexible graphite foil. This in-vessel integration of actively cooled PFCs increased heat removal capacity at least by a factor of 5 compared with the previous HT-7 poloidal limiter. This PFCs with the guard limiter protected LHCD launcher and the improved poloidal feedback control system together have extended the discharge duration from one minute to 4 minutes. A density increase was still observed and limited the discharge duration. In this limiter configuration, however, the SOL plasma became inhomogeneous toroidally due to local short connection length between skipped port space and the density decay length was decreased significantly. This caused the lower density in front of LHCD launcher mouth and coupling of LHW was sensitive to the plasma horizontal position. The LHCD efficiency became lower compared to in the poloidal limiter configuration. In 2005, the limiters were further modified by removing the components between the diagnostic ports. Only two continuous sections at the toroidal positions, corresponding to the iron core of the transformer， were remained, where there are no ports. They cover toroidally 180^o at top and bottom respectively. This modification improves the homogeneity and increase the density decay length of the SOL plasma, which leads to larger wetted area by transported heat on the limiter surface. The peak heat on the limiter surface, thus, is not increased significantly although the area of the limiter surface was reduced. The long pulse discharge up to 6 minutes has been achieved in 2005.

To meet the long pulse operation requirements, several important technical modifications have been made in the last two years. The LHCD control system was improved to provide more flexibility for power feedback control, power modulation, reflection and arc protection. The launcher was protected by an actively water-cooled guide graphite limiter. The new EAST power supplies were tested and replace the original HT-7 poloidal power supplies. The poloidal real-time control system was upgraded with new power supplies from EAST machine and the improved magnetic diagnostics. The current polarity of the new power supplies can be changed during discharges, which provide new capability for the machine operation in AC mode. The new control algorithm was developed to allow the machine operation in AC mode. These modifications have enabled the discharges in different scenarios and to extend discharge duration to 5 minutes, which facilitates the study of some key issues of the steady-state operation. Several new diagnostics including Thomson scattering, CO2 laser collective scattering, charge exchange recombination spectroscopy, IRCCD and a fast reciprocating Langmuir probes provided new capabilities for the plasma physics research.

3. LHCD physics:

HT-7 is an important machine focusing on the long pulse discharges by LH wave. The current drive (CD) efficiency is a key physical issue in evaluating the lower hybrid current drive (LHCD) experiments for long pulse discharges. The fully non-inductive CD efficiency η_0 can be well determined when the loop voltage is zero. With partial current drive, the residual DC electric field applies an additional force on the current carrying fast electrons which can enhance the CD efficiency. For the non-zero loop voltage LHCD discharges, the CD efficiency can be obtained by taking into account the effect of residual electric field on the fast electrons, so called the hot conductivity [9, 10]. The LHCD efficiency was investigated by LHW power scanning at various plasma currents, electron densities and the launched refractive indexes $N_{||}$ of the LHW. The CD efficiency can be determined by fitting the loop voltage variation $\Delta V'/V_{OH}$ against the normalized LHW power $P_{norm}= P_{LH}/\bar{n}_e I_p R$ to:

$$-\Delta V'/V_{OH} = (\eta_0 + \eta_1) P_{norm} / (1 + \eta_1 P_{norm})$$

where $\Delta V'$ is the loop voltage during LHCD phase corrected by plasma conductivity. η_0 is the CD efficiency at zero loop voltage, η_1 is the CD efficiency caused by fast electron hot electrical conductivity and defined as $\eta_1 = \sigma_1 / (P_{norm} \sigma_{sp})$, σ_{sp} is the Spitzer conductivity. It is found that the plots of $\Delta V'/V_{OH}$ against $P'_{norm}= P_{norm}/(5+Z_{eff})$ were same for the line averaged density range up to $1.6\times10^{19}/m^3$, which are fully accessible for all launched $N_{||}$ and density for long pulse discharges in HT-7. The result is shown in Fig. 1. This implies that the difference of the CD efficiency at various densities is mainly due to the effective ion charge predicted by theory. The dependence of the CD efficiency on the various plasma parameters were investigated [11]. The results are summarized in Fig.2 for two launched $N_{||}$. The CD efficiency is almost the linear function of the product of the plasma current and density. It determines the domain of the fully non-inductive current drive in HT-7. The results presented here are similar to but about 30% lower than the previous results in the single poloidal limiter configuration [1]. Possible reason might be due to the much longer magnetic connection length at plasma boundary in the single poloidal limiter configuration, hence better coupling efficiency between LHW and plasma.

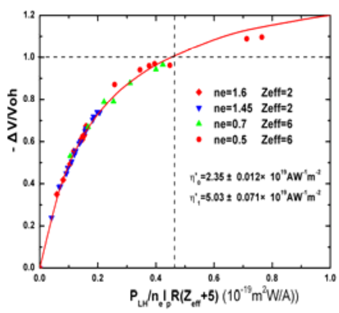

Fig.1 the loop voltage variation against the normalized LHW power for LHCD efficiency estimation

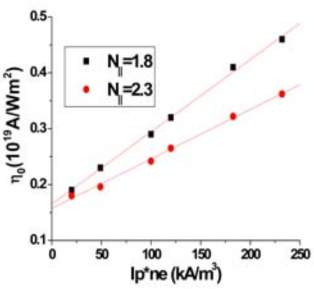

Fig.2 LHCD efficiency as function of $Ip*n_e$ at two launched LHCD $N_{||}^{peak}$

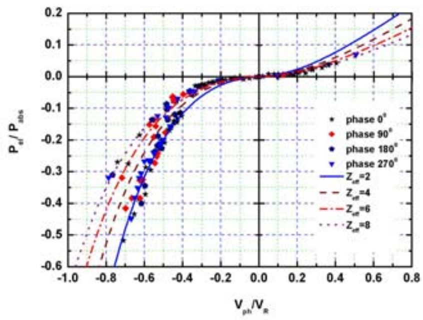

Fig.3 Experimental data of P_{el}/P_{abs} versus V_{ph}/V_R, which are fitted to theory curves with Z_{eff} dependence.

The efficiency of LH waves energy converted to poloidal magnetic field energy has been investigated in extensive parameter ranges in HT-7[12]. The experiments are carried out in the regimes of OH-LH synergy current drive, and current over-drive. The experimental results have been compared with the Karney-Fisch theory [13]. The experimental data confirm theoretical prediction quite well in large range of plasma currents, density, LH waves phase velocities, and LH power as shown in Fig.3. The fitting provide us roughly the $N_{||}$ upshift factor β for different LH phase velocities and the LH wave power absorption fraction α, which is about 0.75 on HT-7. In the regime of transformer recharging experiment, the highest recharging efficiency about 7% has been obtained by current overdrive.

Recently, an m/n=1/1 internal mode in the lower hybrid current driven (LHCD) plasmas has been observed on the HT-7 tokamak [14,15]. As shown in Figure 4, this mode appears during the sawtooth ramp phase, then saturates, damps and finally disappears before the subsequent sawtooth collapse and before the appearance of the precursor oscillations. It occurs between two sawteeth crashes; hence it is named “mid-oscillation” for distinguishing from the precursor oscillation and the post cursor oscillation. It is similar to the ‘partially saturated’ sawteeth found in ECRH experiments on the TCV tokamak [16,17]. However, the m = 1 mode in our experiments was clearer than the one found on TCV, and its amplitude was larger than that of the precursor oscillation. The ‘partially saturated’ sawteeth was reproduced theoretically by introducing the localized heating effect of the ECRH in the island region [17], while the deposition of the lower hybrid wave (LHW) is not localized as that of the ECRH.

The results of singular value decomposition (SVD) of the soft-x-ray signals are shown in Figure 5. It shows that the real frequency and mode structure of the m=1 mode are the same as the sawtooth precursor oscillation. The linear growth rate of the mode is also similar to that of the linear stage of the sawtooth precursor oscillation. However, the growth rate of the precursor increase dramatically just before the sawtooth crash, which may be the reason for the sawtooth crash, while the evolution of the growth rate of the mid-oscillation in the nonlinear stage is similar to that of the external tearing mode in the Rutherford regime [18,19]. The mode usually does not cause the sawtooth crash.

Stability of the mid-oscillation greatly depends on the power deposition location of the LHW and the edge q value [16,17]. The mode is most likely destabilized by the unfavorable plasma current density gradient. The effect of the barely trapped suprathermal electrons can be ignored, according to the obtained threshold condition for electron fishbone. [20]. The stabilizing of the mid-oscillations before the subsequent sawtooth crash and precursor oscillations may result from the flattening of the current profile because of the locally enhanced transport of the suprathermal electrons due to the magnetic island produced by the mid-oscillations. The detailed analysis of the excitation mechanism and stabilization effects was given in another article.

The mid-oscillation usually does not trigger the sawtooth crash, which may suggest that the threshold conditions for the sawtooth crash and the destabilization of the m=1 mode are different. The linear triggering model for sawtooth, proposed by Porcelli *et al.* [21] to predict the sawtooth period on ITER, cannot explain this phenomenon, because the linear destabilization of the m=1 mode is not a sufficient condition for triggering the sawtooth crash in this experiment. The nonlinear activity of the m=1 mode must play an important role in determining the sawtooth crash in this condition. Hence, the linear triggering model is not sufficient to predict the sawtooth crash, and the nonlinear activity of the m=1 mode should also be included.

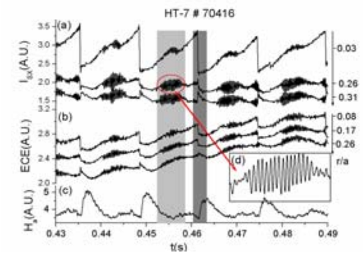

Fig. 4. Temporal evolution of the mid-oscillations and sawteeth oscillations.

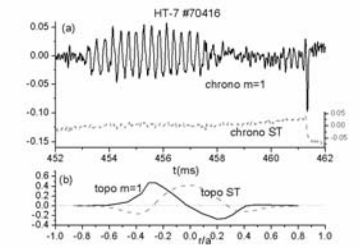

Fig. 5. SVD analysis. (a) the temporal eigenvectors. (b) the corresponding spatial eigenvectors

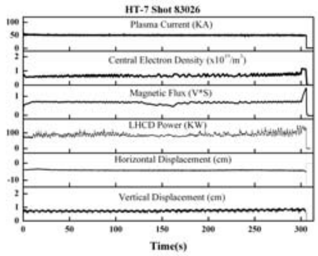

Fig. 6 A long pulse discharge of 306s duration.

4. Long Pulse discharges

A scenario for long pulse discharge of HT-7 uses three proportional feedback loops, which are operated independently of each other. It is similar to the Tore Supra control scenario but not fully identical [22]. The first loop controls the magnetic swing flux of the transformer by varying the lower hybrid (LH) power while a second loop controls the total plasma current through variation of the voltage on the ohmic power supply. The third loop controls the central line averaged electron density by deuterium gas injection using a pulsed piezoelectric valve. During long pulse operation three control loops are used simultaneously for fully non-inductive discharges.

The long pulse discharges were performed follow two main routes. The first route consists of achieving long pulse discharges to address the feasibility of steady states discharges. This scenario was performed by driving the plasma current fully non-inductively through the use of LHCD, which was realized by feedback control of the magnetic swing flux of the transformer at a constant. These techniques has been used to sustain the plasma discharges in HT-7 for 4 minutes at Ip~60 kA, $n_e(0)$~0.8-1×10^{19}/m^3 [7]. In year of 2005, the duration of this operation scenario has been extended to longer than 6 minutes using about 150kW of LHCD, which is the new records of both the pulse length and injected energy in HT-7. The result is shown in Fig.6. The extended discharges qualified the modified PFCs on heat and particle handling capabilities. Unlike the previous experiments, no wall saturation was observed in this shot. There are two main limitations for the pulse length. The first one was different from the previous long pulse discharges, which were caused by uncontrollable density rise due to recycling, but due to the hot spot. The highest surface temperature was observed at ion drift side of the belt limiter on the high field side. The hot spot caused the increase of the carbon influx into the plasma and led the carbon bloom, ultimately terminated the discharge. The surface temperature at the hot spot exceeded the measurable range of the IRCCD, namely > 1000 ^{o}C. The second one was similar to previous experiments, which is caused by uncontrollable density rise due to the outgassing.

The plasmas at the level of Ip~100-120kA, $n_e(0)$~1.5-2.0×10^{19}/m^3 were sustained up to 15 s using 300-500kW of LHCD. The loop voltage was lower than 0.1V. The required LHW power is 500-900kW to achieve full non-inductive current drive at such plasma parameters. This is over the available power under long pulse condition, which limits the pulse length on one hand. On another hand, the recycling caused uncontrollable density rise and terminated the discharge in this case due to the high heat load on the limiter surface. The particles retention, heat load and surface temperature distribution on limiters, and the dust behaviors during the long pulse operation were also studied in these discharges [23-27].

The second route for long pulse discharges operated the machine in AC mode to eliminate the limitation of the maximum available magnetic swing flux in partially non-inductive current drive. LHW and/or ICRF were used to sustain plasma during current spin from one direction to opposite direction. A steady-state AC ohmic plasma discharge up to 53 s has been achieved on HT-7 at the level of Ip=125kA, $n_e(0)$~1.5-2.0×10^{19}/m^3 as shown in Fig.7. There were still plasma density typically at 0.1-0.4x$10^{19}$$m^{-3}$ and radiation power during the plasma current spin, which means existence of the plasma at this time. The plasma density was still under control in such long pulse discharges, while is not possible in continuous operation scenario at the same plasma parameters. The control of the plasma current and position, gas fueling rate, lower hybrid wave power and its deposition and the dynamic real-time feed back control of the magnetic swing flux of the transformer were key issues to achieve steady-state AC operation.

In another operation scenario, LHW was used not only to sustain the plasma during spin of current direction, but also during the flat plateau to drive the plasma current. The co- and counter LHCD, when plasma current was changed from positive to negative, was realized in one discharge. Figure 8 shows a typical discharge. The spin of the plasma current was feedback controlled by the magnetic swing flux of the transformer. Therefore, the available volt-second is same for positive and negative current cycles. Compared to the ohmic discharges, the duration in positive current cycle was longer than subsequent negative cycle at the same LHW power level, corresponding to co- and counter LHCD respectively. The decreased cycle period means an increased loop voltage, and hence decreased LHCD efficiency. This was mainly caused by increased density due to the increased light impurity influxes, mainly, carbon. Details will be discussed elsewhere [28].

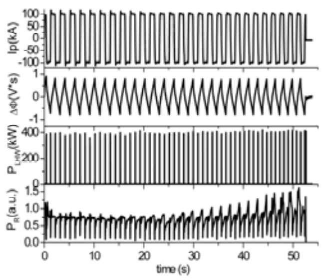

Fig.7 An AC ohmic plasma discharge was sustained for 53 s.

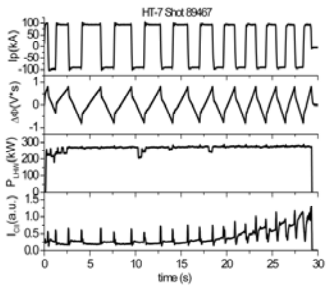

Fig.8 An AC LHCD plasma discharge was sustained for near 30 s.

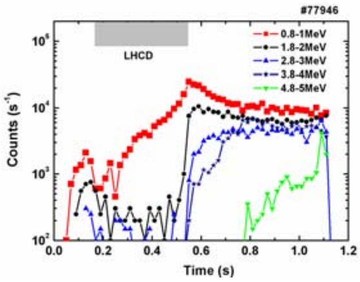

Fig.9 Time slice of forward HXR emission intensity (HXRI) in several energy intervals for discharge No.77946.

5. Behavior of Runaway Electrons

The runaway electrons may be produced in the LHCD plasma and low density plasmas and causes damage of the in-vessel components. They become particularly harmful for long pulse plasmas due to the heat accumulation by impinging on the in-vessel components. The runaway electrons have been measured in combination with hard x-ray detectors and thermo-graphic camera in the HT-7 tokamak [29]. The presence of waves can greatly enhance the runaway production in LHCD plasmas with high residual electric field [30,31]. In runaway discharges, the LH waves may suppress runaway electrons due to the drop of the electric field linked to the non-inductively current drive.

In HT-7, there are two situations for fast electrons to become seed population of runaways. LHCD discharges with high loop voltage as well as the termination of LHW power. In LHCD plasmas with high LH power but non-zero electric field, the fast electron tail can extend above 250 keV. When the LH power was switched off, the loop voltage increased. The fast electron tail was accelerated by electric field over the critical energy and became runaways as shown in Fig.9. While LH waves can suppress the runaways in runaway discharges due to the drop of the electric field below the critical value for electrons to run away [32]. The LHCD reduces the toroidal electric field, which suppressed both the energy and number of runaways. It is efficient for suppression of the energetic runaways. The synchrotron radiation from the runaway electrons monitored by an IR camera in Fig.10 clearly shows that energetic runaways are strongly suppressed and increased when the LH power was turn-on and off respectively.

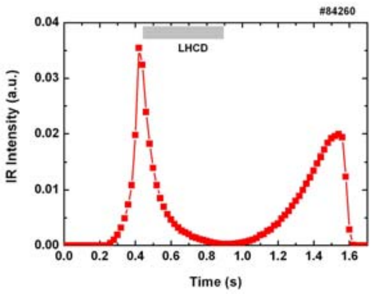

Fig. 10 Time slice of IR intensity for discharge No.84260

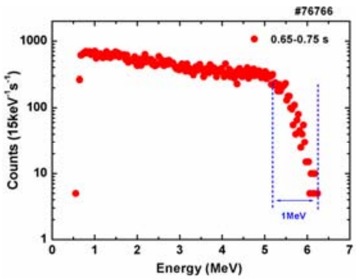

Fig. 11 Typical HXR spectra in runaway discharge

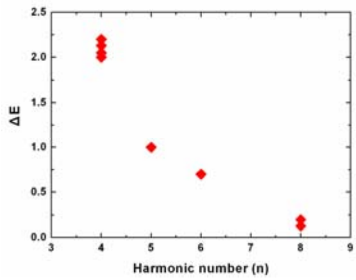

Fig. 12 HXR spectra energy gap for different harmonic number resonance interaction

The energy limit and abnormal energy gap in HXR spectra have been observed in HT-7[33]. The observed maximum energy of the runaways in the edge can not be directly loss of runaways from the core. A dramatic lowering of the energy stems from the resonance of gyromotion with the *n*th harmonic of the magnetic field ripple [34]. The resonance interaction between the electron gyromotion and the ripple will take place at runaway energy of $W_\gamma \approx 30/n$ (MeV) for the typical HT-7 plasmas, where n is the harmonic number. When the runaways accelerated in the toroidal electric field cannot cross a particular ripple resonance, they pile up at this resonance energy as the observed energy gap in the HXR spectra.

The typical HXR spectrum with plasma current 70 kA and the line averaged density $0.5\times10^{19}m^{-3}$ is shown in Fig.11, which shows an abnormal energy gap. The energy cutoff is resulted from the resonance interaction between the runaway electron gyromotion and the fifth harmonic of magnetic ripple. Its value is consistent with the theoretical resonance energy. With decrease of resonance harmonic number, the energy gap (ΔE) is increased. It is shown that, the strength of the resonance increases with decreasing harmonic number [35]. The energy gap at different harmonic number is shown in Fig.12. At the 8th resonance interaction, the energy gap is only 0.2 MeV, while at the 4th resonance interaction, the energy gap increases to 2.05 MeV. Interaction of runaways with magnetic ripple acts an additional barrier to limit the energy of runaways to a few MeVs in the edge, which is favorable to reduce the effect of runaways on first wall during disruptions. By exploiting this virtue, safer operation can be achieved.

6. Edge turbulence

In the recent two years the plasma edge group on HT-7 was devoted to the study of the turbulence structures and their propagation across magnetic surfaces. Some new analysis techniques such as wavelet analysis have been developed and applied to the probe signals [36]. Some of interesting measuring results have been gotten, which are briefly introduced here.
A 12-tip poloidal probe array is used to detect coherent structures in edge plasma turbulence. In order to avoid second electron emission, the experiments are conducted in ohmic discharges at low plasma current, so as to keep the electron temperature at the plasma edge below 50 eV. The turbulence observed in these experiments show typical electron-drift-wave characteristics. In the confinement region they propagate in the electron diamagnetic direction and their frequency is close to the local electron diamagnetic frequency. Their spectra show broad frequency-band and multi wavelength, as indicated in the statistical dispersion relation (figure 13 left). The fluctuation power peaks at low frequency ~ 30 kHz and short wavenumber ~ 1 rad/cm region and decays rapidly towards high-frequency and long-wavenumber region, indicating that the edge plasma turbulence is dominated by the low-frequency and long-wavelength fluctuation components. Since the low-frequency fluctuations have relatively longer wavelength, considerable cross-correlation left at long poloidal distances, as indicated in the three-dimensional cross-correlation spectra (figure 13 right). The correlation length is much shorter in the high frequency region and decays rapidly with the increase of frequency.

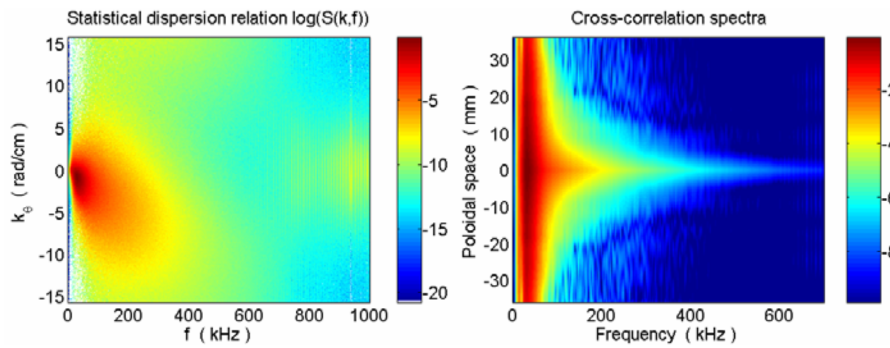

Figure 13 Left: The statistical dispersion relation of the edge plasma turbulence in the poloidal direction. Right: The three-dimensional cross-correlation spectrum of the edge plasma turbulence.

A biorthogonal wavelet is used to extract coherent structures from the plasma turbulence. It is found that there are some large-scale coherent structures within the plasma turbulence. They exhibit very long poloidal extent, even longer than 6 cm, as indicated in figure 14 (a) and (b). Figure 14(a) shows the three-dimensional cross-correlation function and figure 14(b) shows the amplitude of its analytic signal, $\left|\gamma_{analytic}(\tau)\right| = \left|\gamma(\tau) + i\gamma^H(\tau)\right|$, where $\gamma^H(\tau) = \textbf{Hilbert}\{\gamma(\tau)\}$ is its Hilbert transform. These large-scale coherent structures turn into big convection cells. The particle flux driven by these big convection cells is manifested by many intermittent burst events. Due to their high magnitude, long lifetime and big size, the particle transport carried by these large-scale coherent structures can account for up to 50% of the total transport despite their small population (~10% of the events). It is found that these large-scale coherent structures are mainly contributed by low-frequency long-wavelength fluctuating components and their presence is responsible for the observations of long-range correlation, i.e. the correlation in the scale range much longer than the turbulence de-correlation scale.

Besides the large-scale coherent structures, there are also many small-scale coherent structures in the plasma turbulence, mostly contributed by high-frequency short-wavelength fluctuating components, as indicated in figure 14 (c) and (d). They also contribute to transport. All these coherent structures are propagating in the electron diamagnetic direction, driven mainly by E×B drift. The coherent structures are similar in structure between different scales. It is found that the coexistence of these multi-scale coherent structures is responsible for the presence of multi-scale self-similarity in the plasma turbulence.

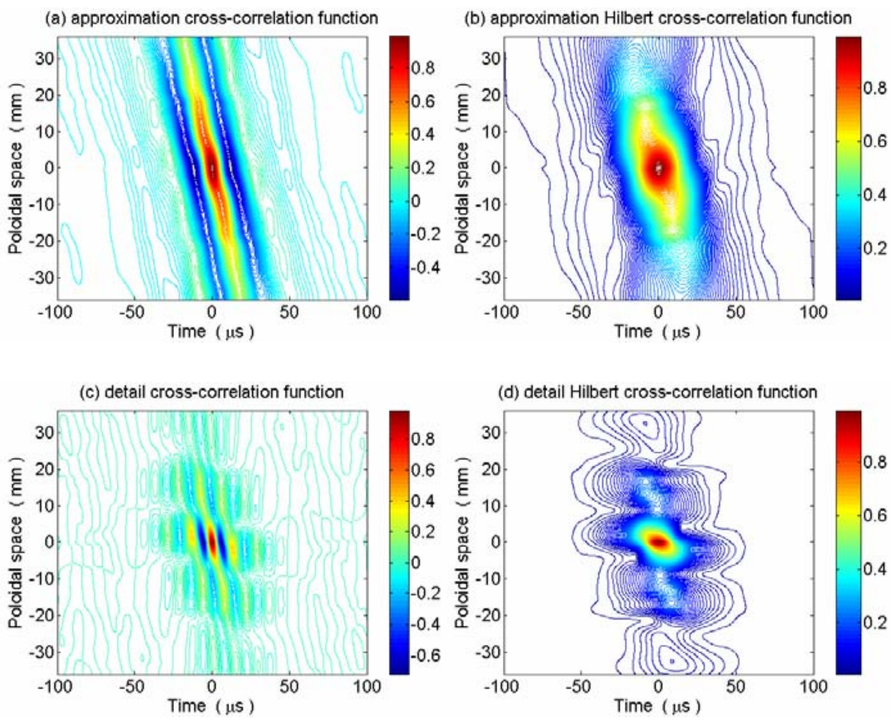

Figure 14. (a) spatiotemporal structure of the large-scale coherent structures, and (b) the amplitude of its analytic signal that corresponds to the large-scale coherent structures; (c) spatiotemporal structure of the small-scale detail structures, and (d) the amplitude of its analytic signal that corresponds to the small-scale coherent structures.

The radial separated Langmuir probes are used to study the propagation of turbulent structures across magnetic surfaces. In confinement region we observed that turbulence propagate outward. with a relative small phase velocity ~ 300 m/s. Radial average wavenumber is 2 ~ 3 rad/cm, which is much higher than the poloidal average wavenumber, as indicated in figure 15. This means that turbulence is dominated by long wavelength components in the poloidal direction, but their radial wavelength is relative short. Radial correlation length is about a half of the poloidal correlation length, which implies that turbulence eddy structures are elongated in the poloidal direction and correlation is stronger within magnetic surface than across the surface. This is possibly due to magnetic shear. These experimental results support the turbulence theory proposed by Mattor and Diamond [37]. They suggested that the radial propagation is a candidate mechanism responsible for driving the edge turbulence by fluctuations in the plasma core region.

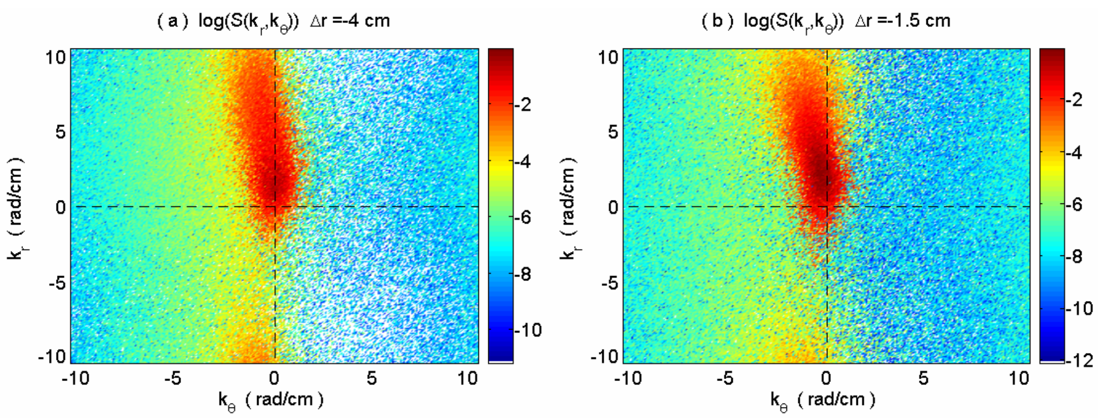

Figure.15 The (k_r,k_θ) double wavenumber spectra of electrostatic turbulence measured by a triple probe array at 4 radial locations: (a) Δr = –4 cm, (b) Δr = –1.5 cm (a = 27 cm)

Particles and heat are carried by these turbulent structures, when they moving outward. Finally they pass through the separatrix and penetrate into the scrape-off layer. Density blobs are generated near the separatrix, we find that the density blobs observed in the scrape-off layer possibly originate from the coherent structure at plasma edge.

In conclusion, in the recent two years the plasma turbulence research on HT-7 is fruitful. Our work is devoted to the understanding of the detailed structures of turbulence and their origin. We will continue in this direction and try to present more observations and detailed comparisons with different models.

7. Summary

In support of the EAST project, HT-7 experiments focused on the long pulse discharges by intensive use of LHCD and relevant physics investigation. The system modifications including the toroidal belt limiter, LHCD control system and protection guide limiter, the real-time poloidal control system with the new EAST power supplies and diagnostics etc are based on the requirements of the long pulse discharge. After these modifications, the plasma discharges were extended up to 306 s at Ip~60 kA, $n_e(0)$~0.8-1×$10^{19}/m^3$, which is the new records of both the pulse length and injected energy in HT-7. The main limitations for discharge duration were uncontrollable density rise or hot spot. In the AC operation scenario, discharges were successfully sustained up to 53 s in ohmic plasma and 30 s in LHCD plasma in the normal HT-7 operation regime. The increased light impurity influxes, mainly, carbon limited the pulse length in these operation modes.

LHCD efficiency based on hot electron thermal conductivity was investigated. It is found that CD efficiency is almost a linear function of the product of Ip*n_e in the central line averaged density up to $1.8\times10^{19}/m^3$ and dependence on the density can be attributed to the effective ion charge as predicted by theory. Investigation of the efficiency of LH waves energy converted to poloidal magnetic field energy confirms the theoretical prediction. In the regime of transformer recharging experiment, the highest recharging efficiency about 7% has been obtained by current overdrive. A new m/n=1/1 internal mode in the lower hybrid current driven (LHCD) plasmas has been observed. This mode appears, saturates, damps during the sawtooth ramp phase and finally disappears before the subsequent sawtooth collapse. The stabilizing of the mid-oscillations before the subsequent sawtooth crash may result from the flattening of the current profile because of the locally enhanced transport of the suprathermal electrons due to the magnetic island produced by the mid-oscillations.

The runaway electrons might be very harmful for long pulse plasma discharges and its behaviors were investigated in HT-7. LH waves can suppress the runaway electrons in runaway discharges due to the drop of the electric field below the critical value for electrons to run away. It is found that the resonance interaction between the electron gyro-motion and the ripple can limit the maximum energy of the runaway electrons in the edge, which is beneficial to safer machine operation.

A 12-tip poloidal rake probe and wavelet analysis was used on the HT-7 tokamak to study intermittently occurring large-scale coherent structures in the edge plasma turbulence. The spatiotemporal patterns of the large-scale coherent structures were reconstructed by using a biorthogonal wavelet. It was found at plasma edge there were some large-scale coherent structures propagating in the electron diamagnetic direction; their poloidal extent was even longer than 6 cm. Analysis indicates these large-scale structures contribute more than 50% of the total outward transport. Radial propagation of electrostatic turbulence was measured using a triple Langmuir probe array in the plasma peripheral region. The experimental results support the turbulence theory proposed by Mattor and Diamond. They suggested that the radial propagation is a candidate mechanism responsible for driving the edge turbulence by fluctuations in the plasma core region.

Acknowledgements

This work was supported by the National Natural Science Foundation of China under Grant No. 10235010 and partially by the Core-University Program of Japanese Society of Promote Sciences.

Reference

[1] Yuanxi, Wan, et al., Nucl. Fusion, 40 (2000) 1057.
[2] Yuanxi Wan, et al., “Overview progress and future plan of EAST Project” OV/1-1, this conference.
[3] J.Jacquinot, Nucl. Fusion **43** (2003) 1583.
[4] H. Zushi, et al. J. Nucl. Mater. **313-316** (2003) 127.
[5] H.Zushi, et al., Nucl. Fusion **45**, (2005) S142.
[6] J.Jacquinot, Nucl. Fusion **45**, (2005) S118.
[7] Baonian Wan, et al., Nucl. Fusion **45**, (2005) S132.
[8] Jiansheng Hu, et al. Fusion Engineering and design 72 (2005) 377-390.
[9] G.Giruzzi, et al., Nucl. Fusion **37**, (1997) 673.
[10] N.J.Fisch, Phys. Fluids 28, (1985) 245.
[11] Chen Zhongyong, et al., Chin. Phy. Lett. 22 (2005) 900

[12] Chen Zhongyong, et al., Chin. Phy. Lett. 22 (2005) 1721
[13] Karney C F, Fisch N J and Jobes F C Phys. Rev. A 32 (1985) 2554
[14] Sun Y., *et al*, Plasma Phys. Control. Fusion **47**, (2005) 745,
[15] Sun Y., et al., The 5th General Scientific Assembly of Asia Plasma & Fusion Association, Jeju, Korea, August 29-31, 2005, TO1
[16] Pietrzyk Z A *et al* Nucl. Fusion **39 (**1999) 587.
[17] Furno I *et al* Nucl. Fusion **41 (**2001) 403.
[18] Rutherford P.H., Phys. Fluids **16**, (1973) 1903,
[19] White R.B. *et al.*, Phys. Fluids **20**, (1977) 800
[20] Sun Y. *et al.*, Phys. Plasmas **12**, (2005) 092507
[21] Pocelli F. *et al.*, Plasma Phys. Control. Fusion **38**, (1996) 2163
[22] T. WIJNANDS, G. MARTIN, Nucl. Fusion 36 (1996) 1201
[23] Hu J. S. et al, “Oxygen wall conditioning for deposits removal and hydrogen releasing on HT-7” 17th conference on plasma and surfcace interaction, May 22-26, 2006, Hefei, China, I-16
[24] Gong X. Z. et al, “Efforts of Particle and Heat Control During Long Pulse Discharges in the HT-7 Tokamak” 17th conference on plasma and surfcace interaction, May 22-26, 2006, Hefei, China, I-6,
[25] Huang J. et al, “Behaviors of Impurity and Hydrogen Recycling in the HT-7 Tokamak” 17th conference on plasma and surfcace interaction, May 22-26, 2006, Hefei, China, O-3,
[26] Lin H. et al, “Temperature Measurements of Limiter Surfaces at High Heat Flux in the HT-7 Tokamak” 17th conference on plasma and surfcace interaction, May 22-26, 2006, Hefei, China, O-15,
[27] Luo G. -N. et al, 17th conference on plasma and surfcace interaction, P2-44
[28] Jiangang Li et al, “Steady-state AC Plasma Current Operation in HT-7 Tokamak” EX/P1-6, this conference
[29] Chen, Z.Y., et al., *Rev. Sci. Instrum.* **77** (2006) 013502
[30] Fisch, N.J., *Rev. Mod. Phys.* **59** (1987) 175,
[31] Liu, C.S. An, Z,G. Boyd, D.A.and Lee, Y.C., Plasma Preprint PL#81-026
[32] Martin-Solis, J.R., et al., *Nucl. Fusion,* **45** (2005) 1524
[33] Zhongyong Chen et al., “Interaction of Runaway Electrons with Magnetic Field Ripple in the HT-7 Tokamak” EX/P3-4, this conference
[34] B.Kurzan, K.H.Steuer, and G.Fussmann, *Phys. Rev. Lett.* **75** 4626 (1995).
[35] J. R. Martin-Solis, B. Esposito, R. Sanchez and J. D.Alvarez, *Phys. Plasmas*, **6** 238 (1999).
[36] Guosheng Xu, et al., “Radial Propagation of Electrostatic Turbulence in the HT-7 Tokamak” EX/P4-33, this conference
[37] N. Mattor, P.H. Diamond, Phys. Rev. Lett. **72** (1994) 486.